Original Paper

phys. stat. sol. (a) **203**, No. 5, 949–955 (2006) / **DOI** 10.1002/pssa.200521118

Deep defect related photoluminescence in heavily doped $CuGaTe_2$ crystals

Andri Jagomägi[*], **Jüri Krustok, Maarja Grossberg, Mati Danilson,** and **Jaan Raudoja**

Department of Materials Science, Tallinn University of Technology, Ehitajate tee 5, 19086 Tallinn, Estonia

Received 27 June 2005, revised 12 January 2006, accepted 10 February 2006
Published online 3 April 2006

PACS 61.72.Ji, 71.55.Ht, 78.55.Hx

$CuGaTe_2$ samples very often exhibit optical and electrical properties of heavily doped semiconductors. This paper investigates the low temperature photoluminescence properties of polycrystalline $CuGaTe_2$ samples. The photoluminescence spectra of "heavily doped" semiconductors are usually characterized by the broadening of the photoluminescence bands that is caused by the fluctuations of the forbidden band edges. The deep photoluminescence region observed (0.8–1.3 eV) consists of two peaks. One of them is located at 0.955 eV and has been reported before. Another, totally new band was discovered at 1.14 eV. The low-temperature j-shift of both bands was detected. Also, rather significant blue shift with the increasing temperature was noticed. It is proposed that both bands consist of two recombination channels. At low temperatures tail-to-impurity recombination dominates. As the temperature increases, the tail-to-impurity recombination transforms into band-to-impurity recombination.

1 Introduction

In recent years much attention has been paid to I–III–VI_2 chalcopyrite compound $CuGaTe_2$ (CGT). This material has the room temperature energy gap $E_g = 1.22–1.24$ eV, which is suitable for solar energy conversion. In addition, its energy gap is direct, it has high optical absorption coefficient, and it is readily made p-type [2–11]. It was found that the complex nature of its pseudo-binary phase diagram leads to the formation of high concentration of intrinsic defects originating from the deviation of its ideal stoichiometry [2, 9]. Therefore wide range of measured E_g and other parameters are reported in the literature. At the same time there are indications that a very shallow acceptor with $E_a \approx 1$ meV is present in this compound [12] and this level often leads to the degeneration of the CGT samples. Probably these shallow acceptor levels are caused by high concentration of acceptors in CGT, see for example [13]. It was shown that the hole gas in CGT is degenerate at hole concentrations above 5×10^{18} cm^{-3}, therefore, due to Burstein–Moss shift, higher E_g values are measured using optical absorption [9, 10]. Another interesting fact is the presence of photoluminescence (PL) bands at higher energy than the lowest band-gap energy of CGT [1, 4, 14]. It was proposed that lower laying valence bands are responsible for these PL bands [4]. The highest valence band in CGT is characterized by three split bands: Γ_7, Γ_6 and Γ_7. This splitting is the result of the combined effect of crystal field and spin–orbit splitting. However, the valence band structure in CGT is not completely understood. Deep photoluminescence (PL) bands in CGT show properties which are difficult to explain using standard PL models for deep PL bands [1]. It was found that the deep PL band at 0.95 eV shows blue shift with increasing temperature and this shift was explained using the model of spatially curved energy gap [1]. All these facts indicate that further studies

[*] Corresponding author: e-mail: andri@kiri.ee, Phone: +372 620 3210, Fax: +372 620 3367

are needed to clarify recombination processes in CGT. In the present work we study the deep PL region 0.8–1.3 eV of polycrystalline CGT samples and present the modernized model of deep level recombination.

2 Experimental

The polycrystalline CGT material was synthesized from 5N-purity components. The phase equilibrium data [1] were taken into account. Cu, Ga and Te were weighted according to the molar ratios 1 : 1 : 2. The materials were loaded into the quartz ampoule, evacuated to high vacuum and sealed. The synthesis proceeded at the temperature of 900 °C in the muffle furnace for 24 hours. Then the ampoule was cooled slowly (0.3 deg/h) in the region of the crystallization point (895 °C to 865 °C) and then with the rate of 10 deg/h to the room temperature. From the analysis of X-ray powder diffraction patterns, the single-phase nature and the chalcopyrite structure of the material were confirmed.

For the PL measurements the samples were mounted into the closed-cycle He-cryostat equipped with the temperature controller that allows to tune the temperature from 8 K to 300 K. Samples were optically excited with the 441 nm He–Cd laser line with the maximum output power of 40 mW. The spectra were recorded via the 40 cm grating computerized monochromator system and detected with the InGaAs or the R-632 photomultiplier detector according to the emission band energy. The emission spectra were corrected according to the grating efficiency variations and the spectral response of detectors.

3 Results

The low temperature deep PL spectrum of our CGT samples is presented in Fig. 1. The edge photoluminescence is presented here just for indication that it exists. The analysis of this part of the spectrum will be presented in following papers. The deep region consists of two bands. The fittings of these bands showed that they are slightly asymmetrical. The lower intensity band A has the peak at 0.955 eV and the higher intensity band B has the peak at 1.14 eV. This kind of broad asymmetric PL bands are very common to heavily doped semiconductors. The temperature dependence of the PL spectra is represented in Fig. 4 and the fitting results in Fig. 5. Both peaks show rather significant shift towards higher energies with increasing temperature (40 meV – A peak, 30 meV – B peak). The laser power dependence of the low temperature PL spectrum revealed strong blue shift with increasing excitation power (j-shift) of both bands. Indeed, in the excitation power range from 3 mW to 40 mW the peaks of A and B bands shifted 10 meV and 5 meV towards higher energies respectively (see Fig. 7).

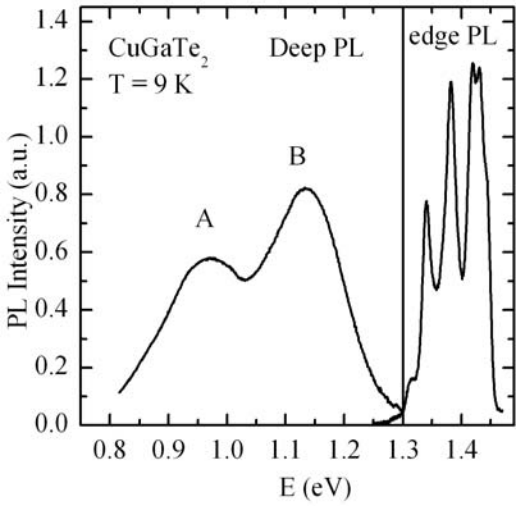

Fig. 1 PL spectrum of polycrystalline CGT samples. The two regions are recorded with two different detectors. The peaks A and B are located at 0.955 eV and 1.14 eV. The detailed study of edge emission will be published in next paper. The fine structure of edge emission implies that our samples were degenerate.

4 Theory

Reference [16] says that the theory of heavily doped semiconductors can be applied to the materials where the main distance between point defects is smaller than the Bohr radius r_b of the defect state ($1/N < r_b^3$, where N is defect concentration). In that case the wavefunctions of the charge carriers that are bound to closely situated defects tend to overlap, giving rise to energy zones instead of distinct defect levels inside the forbidden band. In turn, those zones can reach the edges of the valence and conduction bands and evoke so-called energy tails (see Fig. 2). The forbidden band edges become curved and potential fluctuations emerge. If the fluctuations are strong enough, they can act as potential wells for charge carriers and trap them. Because high concentration of free holes ($>10^{18}$ cm^{-3}), our samples are degenerate. Accordingly, the amplitude of potential fluctuations is strongly reduced by screening. Also, we assume that the effective mass of electrons is small in our samples. Unfortunately, the experimental value of the effective mass of electrons in CGT is not reported in literature. The small effective mass approximation is based on the fact that all chalcopyrite materials tend to have rather small effective masses of electrons [18]. Thus, at the bulk material, there are no potential wells that can trap either electrons or holes. As a result, only exceptionally deep potential wells that are formed by a cluster of defects can localize electrons. Nevertheless, in the presence of deep potential wells, electrons' effective mass is modified compared to that of the bulk material. The actual value is unknown, but we assume that in our material such exceptionally deep potential wells exist and trap electrons at the present value of their effective mass. The location of those wells is probably some defective area of the crystal lattice. There are several origins that can create this kind of deep quantum wells. The defective spot must either attract donor defects or repel acceptor defects. In both cases there emerges a small volume in the lattice, where the electrons' presence is energetically favourable.

In heavily doped semiconductors the recombination between the conduction band and an impurity level can occur via two channels. The first so called tail-to-impurity (TI) recombination takes place between the electrons that are localized in the conduction band tails and the holes that are localized at the acceptor state. The second so-called band-to-impurity (BI) recombination takes place between the free electrons in the conduction band and the holes that are localized at the acceptor state. The theoretical description with computer simulations of the BI-band according to laser power and temperature variations can be found from Ref. [17].

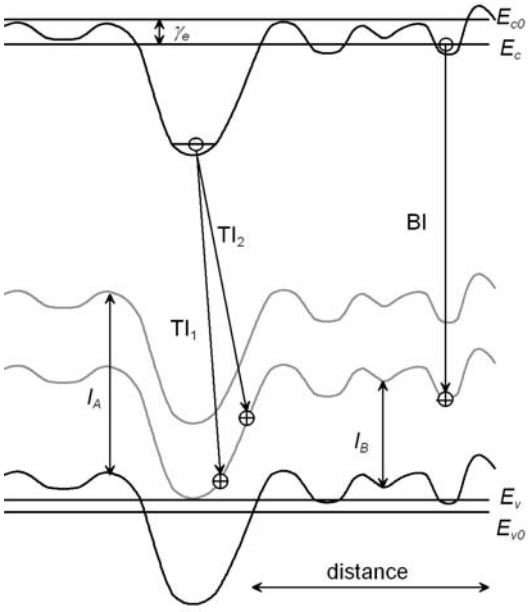

Fig. 2 Band diagram of heavily doped semiconductors. I_A and I_B are the defect level binding energies, E_{c0} and E_{v0} are unperturbed edges of energy gap, E_c is the level of free electrons, and E_v is the level of free holes. The BI band is the result of recombination of free electron and hole that is localised at acceptor state. Some exceptionally deep potential fluctuations act as potential wells for electrons. Inside those wells, electrons have allowed energy states. From those states electrons can recombine with hole that are localised at acceptor states (TI-band). "Vertical transitions" (TI_1) are favoured at higher temperature while "diagonal transitions" (TI_2) are favoured at lower temperature.

Let us now concentrate on the behavior of TI-band. Figure 2 shows that TI-band can exist only if the thermal energy of electrons is not high enough to allow them to escape from the conduction band tails. If not, BI-band can be observed instead of TI-band. Thus, it is expected that as the temperature changes from low to high, TI-band transforms into BI-band. The transition rate depends directly on the depth of the conduction band tails. Thus, the justified question at a given temperature is whether we are observing TI or BI-band. Nevertheless, the TI-band can be easily distinguished from the BI-band. The theory, experiments, and computer simulations in [17] indicate that the maximum of BI-band does not shift according to the laser power variations. On the contrary, the peak position of TI-band should exhibit noticeable j-shift. Namely, because of the localized nature of tail electrons (see Fig. 2), TI transition depends on the hole distance from the potential well; arrows TI_1 or TI_2 in Fig. 2. Because of the higher energy of the involved holes, the TI_1 recombination results in higher photon energy than the TI_2 recombination. Additional relative energy increase comes from the higher Coulomb term in case of TI_1. Namely, the energy of the emitted photon is increased by the Coulomb term that depends respectively on the distance between recombining charge carriers. By its physical nature the Coulomb term is inversely proportional to the charge separation distance. On the other hand, it is known that because of the lower overlapping of the wavefunctions of distant electrons and holes, the recombination of distant pairs saturates faster than the recombination of close pairs. In conclusion, j-shift in case of TI-band should be noticeable. Similarly to the donor-acceptor-pair (DAP) recombination, TI-band shifts towards higher energies with increasing excitation power. The thermal quenching of TI-band can be estimated by the expression [16]:

$$I_{\mathrm{TI}}(T) \propto \exp\left[-(kT \ln \Theta + \gamma_{\mathrm{e}})^{1/2}\ (4(kT)^{-1/2} + \gamma^{-1/2})\right], \tag{1}$$

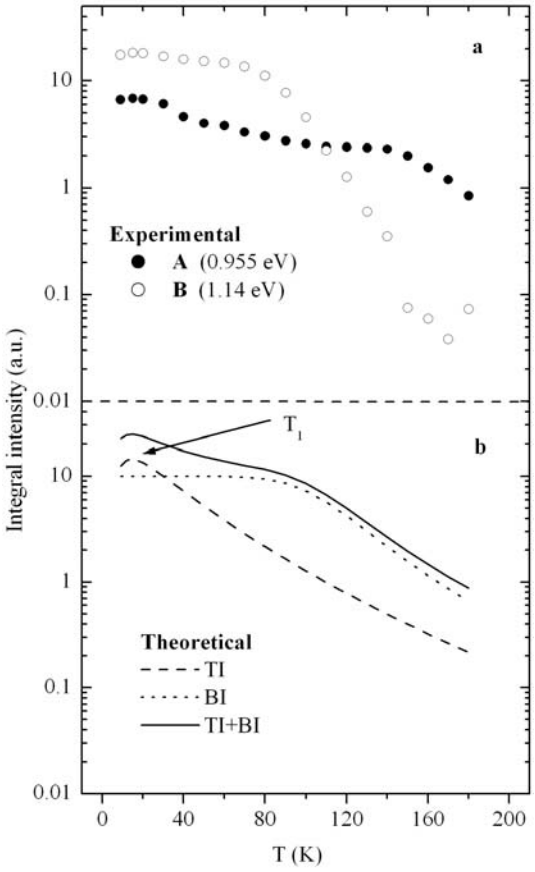

Fig. 3 Integral intensities of A and B bands at various temperatures. Upper graph a) shows the results of fittings of measured PL spectra. Lower graph b) shows the theoretical behaviour of TI + BI bands combined. Both bands, A and B, are dominated by TI recombination at low temeratures. At higher temperatures the intensity of TI band transfers into BI. Integral intensity of TI + BI shows qualitatively very similar behaviour to our measured A and B bands.

where I_{TI} is the integral intensity, Θ is the factor of excitation level i.e. the ratio of the density of electronic states to the density of the generated electrons, $\gamma_e = E_{c0} - E_c$ (see Fig. 2), E_{c0} is unperturbed bandgap edge, E_c is the level where electrons can be considered as free, and γ is the mean-square fluctuation of the potential energy. The shape of the function (1) is shown in Fig. 3b. The intensity of TI-band suffers from both low- and high-temperature quenching, reaching its maximum value at $kT_1 = (16\gamma_e^2\gamma/\ln^2\Theta)^{1/3}$ [16]. The low-temperature quenching is caused by the barrier that holes encounter when physically approaching the potential wells. As a result, at low temperatures the long mean distance between electrons and holes limits the probability of TI recombination. The high-temperature quenching is partially caused by the thermal escape of holes from the impurity level but the main culprit is the thermal liberation of electrons from the conduction band tails. As a result of this process, TI-band simply transforms into the BI-band.

According to [16] the maximum position of TI-band has strong dependence on temperature. The peak position of TI-band can be calculated as:

$$\omega_{max}^{TI} = E_g^0 - \gamma_e - I_a - kT \ln\Theta + 2\sqrt{(kT)^2 \ln\Theta + kT\gamma_e}\,. \tag{2}$$

At very low temperatures ($kT < \gamma_e/\ln^2\Theta$) the maximum of TI-band shifts towards higher energies with the increasing temperature as $\omega_{max}^{TI} \propto 2\sqrt{kT\gamma_e}$. It happens because more TI_1 transitions (see Fig. 2) become available as the additional thermal energy helps holes to approach potential wells. At high temperatures and low excitation values ($\Theta \geq 100$) the kT term in Eq. (2) dominates and ω_{max}^{TI} decreases with increasing temperature. This can be explained as follows. As the temperature increases the shallower tails are emptied first. As a result, the emphasis of the recombinations shifts to deeper tails which holes find more difficult to approach, consequently, less TI_1 transitions become available.

5 Discussion

Figures 4 and 5 show that as the sample temperature increases, the peak position of A and B bands move towards higher energies. At the same temperature range, according to [10], the bandgap energy of CGT exhibits the shift in the opposite direction. This implies that both A and B bands comprise two closely

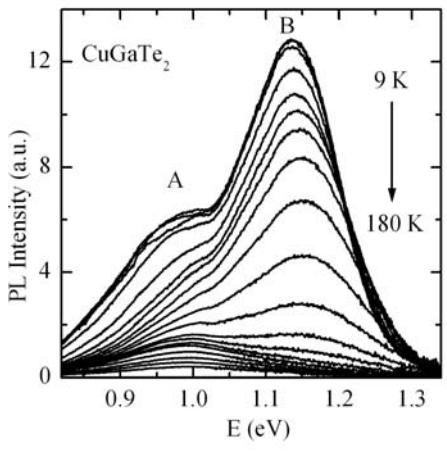

Fig. 4 Temperature dependence of deep PL spectrum of CGT. Both A and B bands show very similar quenching rates. Both bands exhibit considerable blue shift with increasing temperature (see also Fig. 5).

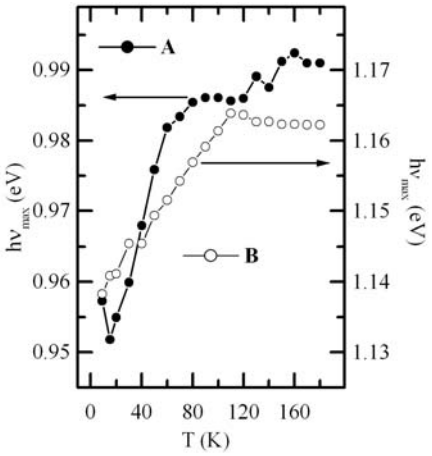

Fig. 5 Temperature dependence of A and B peak positions. In the temperature range from 9 K to 180 K the peak position of band A shifts about 40 meV and the peak position of band B shifts about 30 meV towards higher energies.

situated recombination channels of different origin and the deceptive shift of the peak is actually caused by the transfer of the recombination intensity from one channel to another. We propose that in the present case we see the transition of TI-band into BI-band. However, the involved impurity levels of the A and B bands are different. Accordingly, the activation energies of involved acceptor states are I_A and I_B respectively. Nevertheless, in both cases the shift can be explained as follows. At low temperatures the TI-band, which peak is located at slightly lower energy than the BI-band, prevails. As the temperature increases the PL intensity transfers from TI-band to BI-band. As a result, although the peaks positions of both TI and BI bands are decreasing the peak position of the resulting band (A or B) is moving towards higher energies.

The temperature dependence of intensities of A and B bands, also, the TI and BI bands inside them are depicted in Fig. 3. At low temperatures (below ~30 K) the TI band prevails. Its intensity has its maximum at the temperature T_1. At higher temperatures the BI-band starts to dominate and the behavior of the A and B bands are governed by the quenching of the corresponding BI-band.

Figure 6 shows the Arrhenius plot of the thermal quenching of the A and B bands. The fittings were performed with the semi empiric equation [1, 4]:

$$\Phi(T) = \frac{I_0}{1 + \alpha_1 T^{1.5} + \alpha_2 T^{1.5} \exp\left(-\frac{E_T}{kT}\right)}, \tag{3}$$

where $\Phi(T)$ is integral intensity, I_0 is initial intensity, α_1 and α_2 are the process rate parameters, and E_T is the thermal activation energy. The activation energy $E_T^A = 237 \pm 2$ meV of the band A is most probably caused by the thermal activation of holes from the acceptor state I_A directly into the valence zone. In case of the band B, the quenching process was detected with the activation energy $E_T^B = 90 \pm 1$ meV. The quenching process is caused by the thermal liberation of holes from I_B acceptor state. These values of the activations energies have not been reported before. At this point, there is not enough information to attribute those activation energies to certain defects. The identification of those defects remains for the future studies.

The presence of TI recombination in the bands A and B is confirmed by the laser power dependence of the PL spectrum (see Fig. 7). It was proven in [17] that BI-band does not shift according to excitation

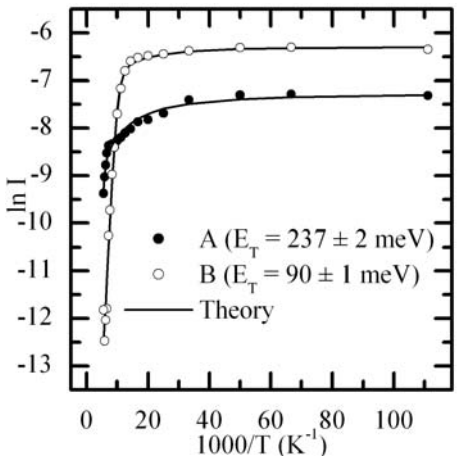

Fig. 6 Fitting results of the thermal quenching of bands A and B. The fittings are performed with Eq. (3).

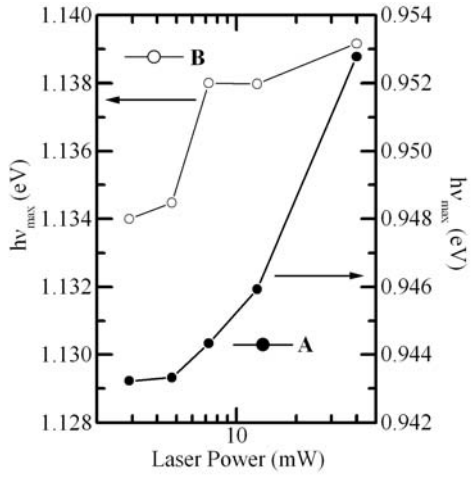

Fig. 7 Laser power dependence of the peak positions of PL bands A and B of CGT. Both bands show rather strong *j*-shift which is common to TI recombination.

power variations. Indeed, the computer simulation showed that the shape and the position of BI-band do not depend on carrier densities. On the contrary our current experiment showed that at 9 K both A and B bands showed rather strong j-shift. As it was described above this shift is specific to TI recombination that j-shifts in similar bases known from DAP recombination.

6 Conclusion

We studied deep PL region (0.80–1.3 eV) of CGT. The region comprises two bands. One of them (at 0.955 eV) has been reported before. The second band (at 1.14 eV) has not been observed before. The similar temperature and laser power dependence of the bands called for similar interpretation. Namely, we use the PL model of heavily doped semiconductors. Though, our samples were not doped intentionally, it is known that CGT and other chalcopyrite compounds tend to have the large concentrations of native defects. In case of heavy doping the forbidden band edges are curved and potential wells (band tails) for electrons and holes are formed. Consequently, new effects that emerge from this localization of electrons and holes can be observed. In the present case, we observed the transformation of "tail-to-impurity" (TI) to "band-to-impurity" (BI) recombination. The band A involves the defect level with higher activation energy than the band B.

Acknowledgement This work was supported by the Estonian Science Foundation, Grant No. 5149.

References

[1] J. Krustok, J. Raudoja, M. Yakushev, R. D. Pilkington, and H. Collan, J. Appl. Phys. **86**, 5305 (1999).
[2] E. I. Rogacheva and O. N. Nashchekina, in: Ternary and Multinary Compounds, Proceedings of the 11th International Conference on Ternary and Multinary Compounds, ICTMC-11 (Institute of Physics Publishing, Bristol, UK, 1998), pp. 159–162.
[3] I. V. Bodnar, V. F. Gremenok, I. A. Viktorov, and D. D. Krivolap, Tech. Phys. Lett. **24**, 89 (1998).
[4] J. Krustok, H. Collan, K. Hjelt, M. Yakushev, A. E. Hill, R. D. Tomlinson, H. Mändar, and H. Neumann, J. Appl. Phys. **83**, 7867 (1998).
[5] A. Rivero, M. Qintero, C. Power, J. Gonzalez, R. Tovar, and J. Ruiz, J. Electron. Mater. **26**, 1428 (1997).
[6] L. Essaleh, S. M. Wasim, G. Marin, E. Choukri, and J. Galibert, phys. stat. sol. (a) **225**, 203 (2001).
[7] C. Rincon, S. M. Wasim, G. Marin, E. Hernandez, and J. Galibert, J. Phys. Chem. Solids **62**, 847 (2001).
[8] P. Guha, S. Roy, S. Chaudhuri, and A. K. Pal, J. Phys. D **35**, 1504 (2002).
[9] G. Marin, G. Sanchez Perez, G. Marcano, S. M. Wasim, and C. Rincon, J. Phys. Chem. Solids **64**, 1869 (2003).
[10] C. Rincon, S. M. Wasim, and G. Marin, J. Appl. Phys. **94**, 2999 (2003).
[11] V. Bodnar, I. A. Victorov, and V. M. Dabranski, J. Cryst. Growth **265**, 214 (2004).
[12] E. I. Rogacheva, in: Ternary and Multinary Compounds, Proceedings of the 11th International Conference on Ternary and Multinary Compounds, ICTMC-11 (Institute of Physics Publishing, Bristol, UK, 1998), pp. 1–14.
[13] H. Neumann, D. Peters, B. Schumann, and G. Kühn, phys. stat. sol. (a) **52**, 559 (1979).
[14] G. Masse, K. Djessas, and L. Yarzhou, J. Appl. Phys. **74**, 1376 (1993).
[15] E. I. Rogacheva, Cryst. Res. Technol. **31**, S1 (1996).
[16] A. P. Levanyuk and V. V. Osipov, Sov. Phys.-Usp. **133**, 427 (1981).
[17] A. Jagomägi, J. Krustok, J. Raudoja, M. Grossberg, M. Danilson, and M. Yakushev, Physica B **337**, 369 (2003).
[18] R. Márquez and C. Rincón, Mater. Lett. **40**, 66 (1999).

